Numerical simulation of fractal conductance fluctuations in soft-wall quantum cavities

Y. Takagaki and K. H. Ploog
Paul-Drude-Institut für Festkörperelektronik, Hausvogteiplatz 5-7, D-10117 Berlin, Germany
(Received 17 February 1999; revised manuscript received 25 May 1999)

Magnetoconductance fluctuations in quantum cavities are numerically calculated for soft-wall confinement potentials. Employing a tight-binding lattice consisting of 200×200 sites, the conductance fluctuations are confirmed to be fractal for one order of magnitude in magnetic-field scale. We find no emergence of self-affine conductance fluctuations with fine scales in a Sinai billiard, suggesting that the hierarchical phase space structure in the underlying classical dynamics alone cannot explain recent experimental observations.

Ever since ballistic electron transport was attained in microcavities fabricated from a two-dimensional electron gas in semiconductor heterojunctions, a considerable amount of effort has been made to uncover novel properties of conductance fluctuations in quantum cavities having chaotic classical dynamics.[1] The most striking feature of the chaotic dynamics is the hierarchical structure in phase space. Recent investigations[2–6] have attempted to associate the self-similar phase-space structure directly with reproducible fluctuation patterns in the conductance.

There are two classes of the self-affinity of the conductance fluctuations. The investigations on one class stem from an experimental observation of hierarchical replications of the fluctuation pattern in Sinai billiards.[2] Theoretically, numerical simulation is the only technique available to examine this remarkable behavior. However, to the best of our knowledge, no one has succeeded in reproducing the experimental observation in a convincing manner.[7] The failure is generally ascribed to limited computational resources. Although the recursive Green's-function method is a powerful technique to calculate the conductance of quantum cavities, the discrete lattice must be fine enough to retain the hierarchical properties in the classical dynamics.

Another class of the self-affinity was first predicted by a semiclassical theory, and is termed fractal conductance fluctuations.[3] The statistical properties of the magnetic-field correlation of the conductance are related to the probability distribution of areas enclosed by electron trajectories in a cavity.[8] The probability distribution decays exponentially for hard-wall cavities, whereas it obeys a power law when the confinement potential of cavities is smooth.[9] The latter is believed to originate from trajectories trapped around the Kolmogorov-Arnol'd-Moser islands in the phase space, which give rise to a long dwell time in the system. The power-law distribution leads to a fractal behavior of the magnetoconductance fluctuations.[3] The fractal dimension D of the conductance fluctuations is predicted[3,10] to be given by the power-law exponent β as $D=2-\beta/2$. Therefore, the theory provides a tool for quantitative analysis of quantum transport in a chaotic system. The theoretical prediction was soon confirmed in experiments.[4–6]

The phenomenon of the fractal conductance fluctuations calls our attention to the importance of the boundary potential. The soft-wall confinement explains a discrepancy in experimental observations:[11] The weak localization conductance peak[12,13] in ballistic cavities around zero magnetic field often behaves as if the dynamics were chaotic although the cavity is made to realize regular dynamics. The confinement potential is inevitably soft in split-gate devices, and so the classical dynamics unintentionally becomes chaotic. Since the soft-wall potential in real devices is generally omitted in theoretical analysis, the drastic influence of the confinement potential signifies a demand for numerical simulations.

In this paper, the magnetoconductance is calculated quantum-mechanically using a lattice model. By increasing the number of lattice sites, we are able to establish the fractal conductance fluctuations for one order of magnitude in magnetic field scale. We also examine the conductance fluctuations when a Sinai diffuser is introduced in the cavity.

We consider a square-shaped cavity, defined in $0<x$, $y<W$, attached by two leads. The cavity and the leads are surrounded by an infinite barrier. A soft-wall potential is assumed within the cavity region. For simplicity, we use a potential determined as a function of the distance in the normal direction from the cavity boundary:

$$U_W(x,y)=u_W\left[\exp\left(-\frac{x}{d}\right)+\exp\left(-\frac{W-x}{d}\right)+\exp\left(-\frac{y}{d}\right)+\exp\left(-\frac{W-y}{d}\right)\right]. \tag{1}$$

The soft-wall potential is set to be absent for part of the cavity boundary where the leads are attached (Fig. 1). The cavity is simulated by a square lattice with 200×200 sites, unless stated otherwise. To avoid peculiarities that may arise when the device geometry is symmetric, the two leads are assumed to be nonidentical. One lead with width $\frac{18}{201}W$ is attached at $0.65<y/W<0.74$ and the other with width $\frac{21}{201}W$ is attached at $0.7<x/W<0.8$. The conductance is calculated using the lattice Green's-function technique.[14]

Let us first investigate the classical dynamics in the model cavity potential. The electron trajectory is gradually deflected from the boundary by a force $\mathbf{F}(x,y)=-\boldsymbol{\nabla}U_W(x,y)$. We solve Newton's equation numerically using a predictor-corrector method:[15]

$$\mathbf{x}(i+1)=\mathbf{x}(i)+\mathbf{v}(i)\Delta t+\mathbf{F}(\mathbf{x}(i))(\Delta t)^2/(2m), \tag{2}$$

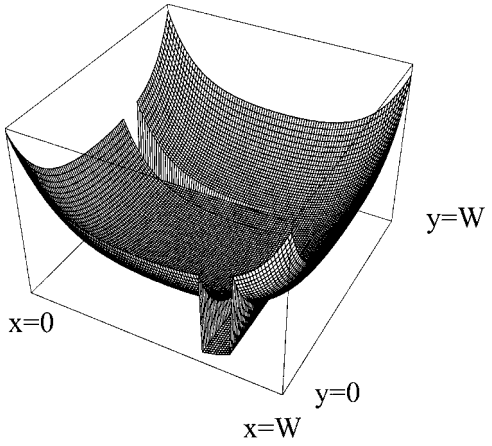

FIG. 1. Cavity potential U_W with a soft-wall confinement. The decay length d of the boundary potential is 0.12W. The width of the leads is $\frac{18}{201}W$ and $\frac{21}{201}W$.

$$\mathbf{v}(i+1)=\mathbf{v}(i)+\{\mathbf{F}(\mathbf{x}(i))+\mathbf{F}(\mathbf{x}(i+1))\}\Delta t/(2m), \quad (3)$$

where $\mathbf{x}(i)=(x(i),y(i))$ and $\mathbf{v}(i)$ are the position and the velocity of an electron at the ith time step of period Δt. The accuracy of the numerical calculation was checked by monitoring the energy conservation. In the inset of Fig. 2, we show an example of chaotic trajectories trapped in the cavity. The probability $P(t)$ to stay in the cavity for a time longer than t decays algebraically, as shown in Fig. 2, with the power-law exponent 1.6. The deviation from the power-law behavior for small t is due to direct trajectories between the leads. In the large-t regime, the probability distribution rather obeys an exponential behavior, which is a remnant of that in a hard-wall cavity.

The curves labeled a and b in Fig. 3 show the quantum-mechanical conductance for hard- and soft-wall potentials, respectively. Here, $\phi_0=h/e$ is the magnetic flux quantum. The electron energy is $-3.7t$ with t being the nearest-neighbor hopping amplitude, and so the ratio between the cavity width and the Fermi wavelength is $W/\lambda_F=17.5$. This value is chosen to correspond to the devices examined in Refs. 2 and 4. In both leads, three transverse modes are occupied. The electron injection properties thus are considered to be fairly classical.

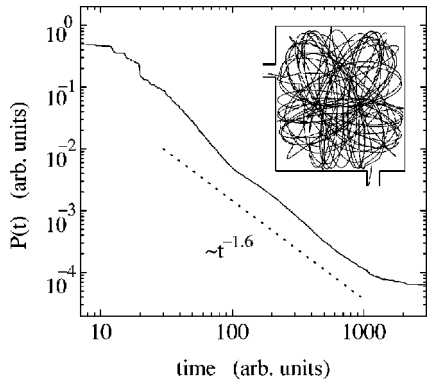

FIG. 2. Classical probability $P(t)$ of an electron to stay in a cavity with $d=0.12W$ longer than a time t in a perpendicular magnetic field that corresponds to $BW^2=10\phi_0$ in Fig. 3. The inset shows a chaotic trajectory trapped in the cavity.

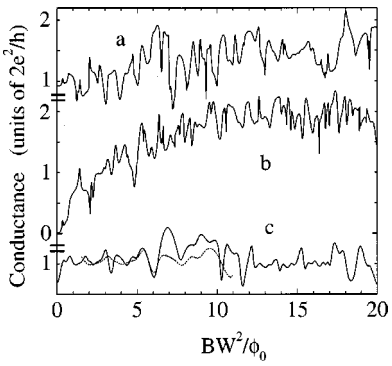

FIG. 3. Magnetoconductance for the hard-wall cavity (curve a), soft-wall cavity (curve b), and soft-wall cavity containing an antidot (curve c). The dotted line shows curve c with the magnetic-field scale multiplied by a factor 1.79. For curve b, $u_W=0.3t$, $d=0.12W$. For curve c, $u_W=u_S=0.3t$, $d=0.025W$, $r_0=0.547W$, $x_0=0.515W$, $y_0=0.525W$.

A fractal analysis of the conductance fluctuations is carried out in Fig. 4. We use the same ''box-counting'' algorithm described in Ref. 4. The magnetic-field range is divided with an interval ΔB. The difference of maximum and minimum conductance values within the interval is summed over the whole segments. The number of boxes $N(\Delta B)$ is given by dividing the sum by ΔB. As indicated by the solid line, a power-law behavior is found over one order of magnitude of the magnetic-field scale for the soft-wall cavity (circles). For the hard-wall cavity (triangles), the slope keeps decreasing for smaller ΔB. The fractal dimension for the soft-wall cavity is $D=1.35\pm0.05$. The value of D we obtained in our numerical simulation is incidentally in good agreement with the experimental observation.[4] However, we do not attempt to make a comparison with the experiment as the actual confinement potential that determines the fractal dimension is unknown.

We observe deviations from the power-law behavior for both small and large ΔB. The deviation for large ΔB is due to the loss of correlation. Since the conductance fluctuations

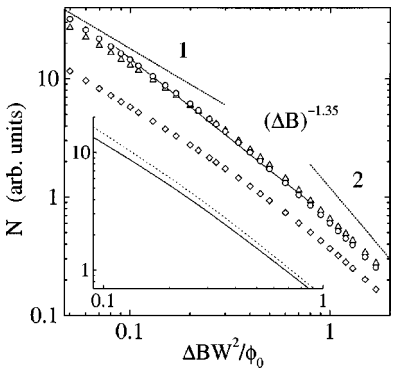

FIG. 4. Fractal analysis for the conductance fluctuations plotted in Fig. 3. Triangles, circles, and diamonds correspond to the curves a (hard wall), b (soft wall), and c (Sinai billiard), respectively. The dotted lines show the slopes when the power-law exponent is 1 and 2. The solid line is a guide for eyes, giving the fractal dimension $D=1.35$. The inset shows the number of boxes N for the soft-wall cavity. The solid and dotted lines are obtained using 100×100 and 200×200 lattices, respectively.

are uncorrelated when the magnetic flux piercing through the cavity is changed by more than one flux quantum, the fractal dimension approaches 2 when $\Delta B W^2/\phi_0 > 1$. The deviation for small ΔB is attributed to the limited number of lattice sites. In the inset of Fig. 4, $N(\Delta B)$ evaluated using 100×100 and 200×200 lattices is shown by solid and dotted lines, respectively. The device parameters are scaled accordingly so that the potential profile is identical with respect to the Fermi wavelength, apart from differences arising from the discrete lattice. The energy is, for example, $-2.8t$ for the 100×100 lattice. Although the dependence of N on ΔB is closer to the power-law behavior in comparison to that for a hard-wall cavity, the power-law dependence is restricted to a narrow range of ΔB when the number of lattice sites is reduced. For the 200×200 lattice, the fractal dimension becomes 1 for $\Delta B W^2/\phi_0 < 0.06$, indicating the absence of conductance fluctuations in this magnetic-field scale. We emphasize that the curves in Fig. 4 always exhibit upward bowing as the slope in small and large magnetic-field scales is fixed to be 1 and 2, respectively. Therefore, the fractal behavior can be judged quite rigorously.

Assuming that the power-law exponents for the dwell time and for the enclosed area are identical,[3] $D=1.2$ is expected from the classical simulation. There are several possible explanations for the relatively large disagreement of D. In the quantum-mechanical calculation, hard-wall potentials are assumed outside of the cavity. These boundary potentials do not influence the classical trajectories. The electron wave function, however, is expelled from the periphery of the cavity. This may also be part of the reason the fractal behavior is limited to over one order of magnitude of ΔB. As the limited number of lattice sites restricts the power-law behavior to a narrow range of ΔB, the number of lattice sites needs to be increased further for detailed comparison with classical simulations.

Having demonstrated that the number of lattice sites is large enough to generate the fractal conductance fluctuations, we next examine the conductance of a Sinai billiard. We place in the cavity an antidot potential

$$U_S(x,y) = u_S\left[1+\cos\left(\pi\frac{r}{r_0}\right)\right]^4, \tag{4}$$

which is defined for $r \equiv \sqrt{(x-x_0)^2+(y-y_0)^2} < r_0$. When the diameter of the antidot potential is increased, the magnetoconductance exhibits a regular oscillation with period $\delta(BW^2/\phi_0)\approx 1$ (curve c in Fig. 3), in agreement with the experimental observation.[2] The oscillation is expected to be due to the Aharonov-Bohm effect. As the Aharonov-Bohm loop is not explicitly defined in the cavity geometry, periodic oscillations emerge only if the constrictions created between the antidot and the cavity boundary transmit least number of modes. Taylor *et al.*[2] observed that the quantum interference structure was hierarchically repeated with reduced scales when magnetic field approached zero. In contrast to the experiment, however, fluctuations with scales smaller than those in the absence of the antidot do not appear in our numerical results. On the contrary, the fluctuations with fine scales tend to be suppressed for large antidot diameters. The suppression is plausible because of the reduced number of cavity modes, which results in less evolved mode-mixing effects.

Similar problems are experienced when the width of the lead is varied. On the one hand, resonance features are pronounced when the lead is narrow, as the level broadening induced by the lead is suppressed. They may lead to conductance fluctuations with smaller magnetic-field scales. On the other hand, reducing the lead width also decreases the number of occupied modes in the lead. Fluctuations with fine conductance scale are eliminated when there are only a few modes in the leads. This can be understood by considering the fact that the conductance fluctuations consist of transmission resonances with unity amplitude, in units of $2e^2/h$, when the cavity is terminated by single-mode leads. (The unity amplitude is achieved provided that the system is symmetric.)

Nevertheless, the conductance occasionally develops self-affine-like fluctuations. The curve labeled c in Fig. 3 is an example where the conductance fluctuations appear to contain a self-affinity.[16] However, because of the above-mentioned reason, the self-affinity, if indeed present, takes place in large magnetic-field scales. In the experiment by Taylor *et al.*,[2] a replica of the fluctuation pattern was observed near zero magnetic-field with the magnetic field scale by about a factor of 20 smaller than the original. However, it should be stressed that there is no reason to observe the exact similarity nor a particular magnification factor since the phase-space structure of the Sinai billiards, which is expected to be responsible for the exact similarity, is merely self-*similar*. In this respect, the fluctuation pattern in curve c is self-similar. The self-similarity is recognized for several magnification factors, and because of that the fluctuation pattern does not show the exact similarity. We show the best case by the dotted line, for which the magnetic field is multiplied by 1.79. Therefore, our numerical result suggests that the experimental observation in the Sinai geometry cannot be explained by the self-similarity of the underlying classical dynamics alone. However, since the conductance fluctuations are fractal in our simulation merely over one order of magnetic-field scale, it is possible that the lattice is not fine enough to resolve the exact self-affinity. As a matter of fact, the fluctuation pattern in curve c is not fractal as shown in Fig. 4 despite the soft-wall potential. This is probably due to the relatively large antidot size. (The diameter of the antidot potential at the Fermi level is $r_0 = 0.547W$.) Placing an antidot in the middle of the cavity reduces the conduction area of electrons, resulting in less developed chaotic behavior. The reduction may be critical when the lattice system is barely able to produce the fractal conductance fluctuations. To secure a comparable conduction area, the cavity has to be made larger in accordance with the antidot size. The number of lattice sites to investigate unambiguously the exact self-affinity hence needs to be considerably larger than that for the fractal conductance fluctuations. Nevertheless, with the 200×200 lattice, we observe no sign of fluctuations with fine scales in the vicinity of zero magnetic field for various antidot potentials we examined.[17]

In conclusion, we have numerically examined the conductance fluctuations in quantum cavities. When the lattice is fine enough, the fluctuation pattern is found to be fractal for

soft-wall cavities. The upper bound of the magnetic-field scale for the fractal behavior occurs when the magnetic field is varied by more than one flux quantum threading through the cavity. In numerical results, the lower bound is set by the coarseness of the lattice. Despite the successful observation of the fractal conductance fluctuations, the nonstatistical self-affinity in Sinai billiards is not found in our numerical results.

[1] For a review, see Chaos Solitons Fractals **8** (7/8) (1997).

[2] R.P. Taylor, R. Newbury, A.S. Sachrajda, Y. Feng, P.T. Coleridge, C. Dettmann, N. Zhu, H. Guo, A. Delage, P.J. Kelly, and Z. Wasilewski, Phys. Rev. Lett. **78**, 1952 (1997); R.P. Taylor, A.P. Micolich, R. Newbury, and T.M. Fromhold, Phys. Rev. B **56**, 12 733 (1997).

[3] R. Ketzmerick, Phys. Rev. B **54**, 10 841 (1996).

[4] A.S. Sachrajda, R. Ketzmerick, C. Gould, Y. Feng, P.J. Kelly, A. Delage, and Z. Wasilewski, Phys. Rev. Lett. **80**, 1948 (1998).

[5] A.P. Micolich, R.P. Taylor, R. Newbury, J.P. Bird, R. Wirtz, C.P. Dettmann, Y. Aoyagi, and T. Sugano, J. Phys.: Condens. Matter **10**, 1339 (1998).

[6] H. Hegger, B. Hackestein, K. Hecker, M. Janssen, A. Freimuth, G. Reckziegel, and R. Tuzinski, Phys. Rev. Lett. **77**, 3885 (1996).

[7] R. Akis and D.K. Ferry, Physica B **249-251**, 368 (1998).

[8] R.A. Jalabert, H.U. Baranger, and A.D. Stone, Phys. Rev. Lett. **65**, 2442 (1990).

[9] Y.-C. Lai, R. Blümel, E. Ott, and C. Grebogi, Phys. Rev. Lett. **68**, 3491 (1992).

[10] B.B. Mandelbrot, *The Fractal Geometry of Nature* (Freeman, San Francisco, 1982).

[11] J.P. Bird, D.M. Olatona, R. Newbury, R.P. Taylor, K. Ishibashi, M. Stopa, Y. Aoyagi, T. Sugano, and Y. Ochiai, Phys. Rev. B **52**, 14 336 (1995).

[12] H.U. Baranger, R.A. Jalabert, and A.D. Stone, Phys. Rev. Lett. **70**, 3876 (1993).

[13] A.M. Chang, H.U. Baranger, L.N. Pfeiffer, and K.W. West, Phys. Rev. Lett. **73**, 2111 (1994).

[14] H.U. Baranger, D.P. Di Vincenzo, R.A. Jalabert, and A.D. Stone, Phys. Rev. B **44**, 10 637 (1991); T. Ando, *ibid.* **44**, 8017 (1991).

[15] T. Yamada and D.K. Ferry, Phys. Rev. B **47**, 1444 (1993).

[16] In calculating curve *c*, the barrier collimation effect [C.W.J. Beenakker and H. van Houten, Phys. Rev. B **39**, 10 445 (1989); Y. Takagaki and D.K. Ferry, *ibid.* **45**, 13 494 (1992)] is taken into account by gradually increasing the bottom potential in the lead by $0.05t$ while leaving away from the cavity. As a consequence, the number of occupied modes in the lead is reduced to 2. We find, however, no appreciable difference in the fluctuation characteristics due to the collimation effect.

[17] The computation speed can be drastically improved if the cavity potential can be split into identical segments. The size of the matrix that we have to deal with to calculate the lattice Green's function is determined by the number of transverse lattice sites. Therefore, the Green's function of a decomposed segment is calculated much faster than that of the whole system. Taking advantage of the identity of the potential, the Green's function of the rest of the segments can be calculated using gauge transformation. The Green's function of the system is obtained from that of the decomposed segments by restoring the bonds between the segments. We employed this method by dividing the antidot device into four components at $x=y=W/2$. (The confinement potential has to be modified to satisfy the identity.) Although we calculated the magnetoconductance using a 500×500 lattice, the self-affine fluctuations were not found.